Distribution Agreement

In presenting this thesis or dissertation as a partial fulfillment of the requirements for an advanced degree from Emory University, I hereby grant to Emory University and its agents the non-exclusive license to archive, make accessible, and display my thesis or dissertation in whole or in part in all forms of media, now or hereafter known, including display on the world wide web. I understand that I may select some access restrictions as part of the online submission of this thesis or dissertation. I retain all ownership rights to the copyright or the thesis or dissertation. I also retain the right to use in future works (such as articles or books) all or part of this thesis or dissertation.

Signature:

_____ _____

Erin Price Date

Novel aptamer-based detection and sequestration techniques of small molecule toxins

By

Erin Price
B.S., University of Utah, 2017

Chemistry

_____
Jennifer Heemstra, Ph.D.
Advisor

_____
Vincent Conticello, Ph.D.
Committee Member

_____
Stefan Lutz, Ph.D.
Committee Member

Accepted:

_____
Lisa A. Tedesco, Ph.D.
Dean of the James T. Laney School of Graduate Studies

_____
Date

Novel aptamer-based detection and sequestration techniques of small molecule toxins

By

Erin Price
B.S., University of Utah, 2017

Advisor: Jennifer Heemstra, PhD

An abstract of
A thesis submitted to the Faculty of the
James T. Laney School of Graduate Studies of Emory University
in partial fulfillment of the requirements for the degree of
Master of Science
in Chemistry
2020

Abstract

Novel aptamer-based detection and sequestration techniques of small molecule toxins

By Erin Price

Small molecules are important compounds that exist in almost every facet of life and have many functional classes such as drugs, toxins, biomarkers, nutrients and metabolites. Depending on the structure and context, small molecules can have beneficial or harmful effects. However, detection of small molecules is difficult because of their size and limited functional groups. One promising technique to detect small molecules is the use nucleic acid aptamers. Aptamers are single stranded nucleic acid sequences with high affinity to a target molecule. The work in this thesis builds upon current aptamer technology to improve detection and sequestration of small molecule toxins. One area of research will focus on the detection of a small molecule toxin by developing an aptamer-based fluorescent biosensor. The next area of research will combine aptamers and virus-like particles for the sequestration of a small molecule toxin.

Novel aptamer-based detection and sequestration techniques of small molecule toxins

By

Erin Price
B.S., University of Utah, 2017

Advisor: Jennifer Heemstra, PhD

A thesis submitted to the Faculty of the
James T. Laney School of Graduate Studies of Emory University
in partial fulfillment of the requirements for the degree of
Master of Science
in Chemistry
2020

Acknowledgements

This graduate work would not have been possible without the immense support and encouragement from many mentors, family, and friends. I would first like to thank my advisor, Professor Jen Heemstra, for her unwavering support throughout my graduate program. I am grateful for her mentorship and career advice that has been invaluable to my personal and scientific growth. She played a significant role in shaping me into the scientist I am today and never stopped supporting me.

I would also like to thank my committee members, Professors Vincent Conticello and Stefan Lutz, for their time, guidance, and encouragement during my time at Emory University. Additionally, Emory University and the Laney Graduate School have been conducive to facilitating my education and providing me with financial support. I also appreciate my mentors at the University of Utah, Professors Joel Harris and Peter Flynn, for the critical role they played in my development at the University of Utah.

I am also very grateful for the past and current members of the Heemstra lab who have inspired me to grow and improve every day: Dr. Brad Green, Dr. Alex Rangel, Dr. Zhesen Tan, Dr. Hershel Lackey, Dr. Travis Loya, Teworedos Aleye, Colin Swenson, Steve Knutson, Misael Romero, Aimee Sanford, Hector Argueta-Gonzalez, Rachel Bender, Brea Manuel, and Diane Karloff. I am especially grateful for Brad Green, Zhesen Tan, and Hershel Lackey for their friendship, mentorship, and laboratory comedy.

Most of all, I forever grateful for my incredible family, who has always supported me and helped me to attain my dreams through unconditional love. Finally, I would like to thank Brian for all the fantastic adventures and support throughout my educational career.

I couldn't have done it without every one of you.

TABLE OF CONTENTS

List of Figures **Page**

List of Tables **Page**

List of Abbreviations

aa	amino acid
BHQ1	black hole quencher 1
C°	Celsius degree
CCMV	cowpea chlorotic mottle virus
DNA	2'-deoxyriboucleic acid
FAM	fluorescein
FANA	2′-deoxy-2′-fluoroarabinonucleic acid
g	gram(s)
His	histidine
HRV	human rhinovirus
K_D	dissociation constant
kDa	kilo dalton
lys	lysine
min	minute
mM	millimolar
Mol	moles
MP	mutant protein
nM	nanomolar
nm	nanometer

nt	nucleotide
OTA	ochratoxin a
PAGE	polyacrylamide gel electrophoresis
PBS	primer binding site
PCR	polymerase chain reaction
RNA	ribonucleic acid
SDS	sodium dodecyl sulfate
SEC	size exclusion chromatography
SELEX	systematic evolution of ligands by exponential enrichment
SS	structure switching
TEM	transmission electron microscopy
VLP	virus-like particle
XNA	xeno nucleic acid

Chapter 1: Introduction and Background

Small Molecules

Small molecules (<900 g/mol) are low molecular weight organic compounds that affect key biological processes.[1] These molecules have several functional classes such as drugs, toxins, biomarkers, nutrients, and metabolites, which can have beneficial or harmful effects depending on structure and context.[1] For example, in medicine, small molecules serve as antibiotics and disease biomarkers;[2] in agriculture, they function as pesticides and toxicants;[3] and in scientific research, they are used as catalysts and reagents.[4] This extensive involvement of small molecules in everyday life accentuates the need for developing a robust approach for their identification, sequestration, and controlled release.

Although the importance of small molecules is known, detection and sequestration systems have been slow to emerge. There are several reasons for this, including the small surface area and the unique structural properties of each molecule.[5] In general, small molecules have limited functional groups, which makes them difficult to immobilize and generate detection platforms.[6] There are two primary affinity-based detection approaches: antibodies and nucleic acid aptamers.[7] Antibodies are proteins that have an affinity for a specific molecule and are the gold standard.[6] These biomolecules are produced by triggering the immune system and are extracted from living animals for research purposes. However, this mechanism of production limits their broader applicability for small molecules that are non-immunogenic or highly toxic to the host organism.[8] Therefore, over the last twenty years, nucleic acid aptamers have been gaining interest in the scientific community as a more specific and affordable alternative to antibodies.[9] Aptamers are single stranded oligomers that are selected *in vitro* to have high affinity and selectivity to a specific

target molecule.[10,11] The *in vitro* selection process allows for production of aptamers against toxic compounds.[12] Additional advantages of aptamers over conventional antibodies include being less expensive, having less batch-to-batch variability, being thermally stable, and easily modifiable.[13] The ease of manipulation and the unique structure of aptamers also makes them more effective than antibodies at distinguishing subtle structural differences in small molecules.[14,15]

The work in this thesis document, supported by the Heemstra lab, focuses on aptamers for the detection and sequestration of small molecule toxins. Aptamers are selected through an *in vitro* process called the Systematic Evolution of Ligands by EXponential Enrichment (SELEX) (Figure 1.1).[16–18] This three-step process includes selection, elution, and then amplification. First, the target is immobilized on a solid support and incubated with a random DNA library containing known primer binding sites. Following incubation, unbound DNA sequences are removed and bound functional sequences are eluted from the immobilized target molecule. These functional sequences are then amplified through PCR and denatured on PAGE for sequence separation. The selection process is repeated until a DNA sequence with high affinity to the target molecule is isolated.

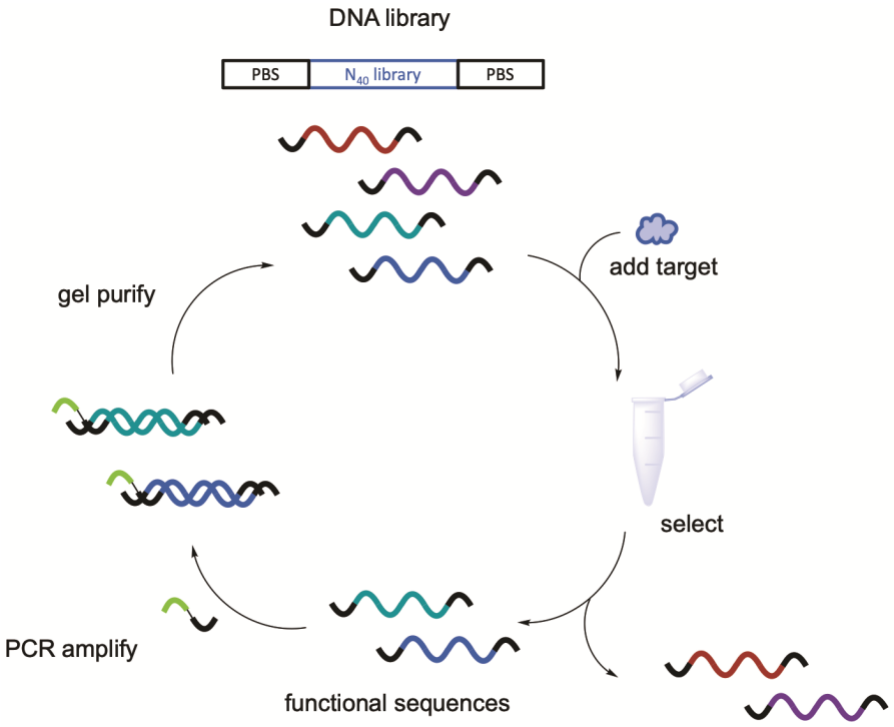

Figure 1.1. General SELEX scheme. A random DNA library is incubated with immobilized target molecule. Unbound sequences are washed away, functional sequences are eluted off and then PCR amplified. The amplified functional sequences are gel purified for the next round of selection.

This well-established approach has developed aptamers for a wide range of applications, including proteins, cells, drugs, hormones, and toxins.[19] My thesis will focus on the two aptamer-based approaches for detection and sequestration of a small molecule toxin. One area of research as described in Chapter 2 focused on the detection of a small molecule toxin by developing an aptamer-based biosensor. A second research thrust is described in Chapter 3 and focused on the sequestration of a small molecule toxin using a combined aptamer and virus-like particle system.

Small molecule detection with TNA aptamer-based biosensor

Biosensors are assays or devices that recognize a biological interaction that can be translated into a readable output such as fluorescent, optical, electrical, or electrochemical outputs.[20,21] Biosensors that can detect small molecules have many important applications, including RNA imaging, medical diagnostics, and drug and toxin detection.[22,23] DNA aptamer-based biosensors are an ideal approach because they are generated for a wide variety of molecules with high sensitivity and specificity. However, DNA aptamers are unusable for many biological applications.[24] DNA aptamers are highly susceptible to nuclease degradation, a common component of biological systems, because they are hydrophobic and have an overall negative charge.[25,26]

To overcome this limitation, groups have utilized xeno-nucleic acids (XNA), which can provide nuclease resistance and increased stability in biological fluids and intracellular environments.[27,28] XNAs are not as susceptible to nuclease degradation because of their modified backbones (Figure 1.2).[27] There are variety of XNAs that have been used to develop XNA aptamers, for example the DeStefano lab used 2'-deoxy-2'-fluoroarabino nucleic acid (FANA) to develop an aptamer with picomolar affinity to HIV-1.[29] The Keefe lab developed an aptamer for vascular endothelial growth factor (VEGF) using 2'-O-Methyl RNA.[30]

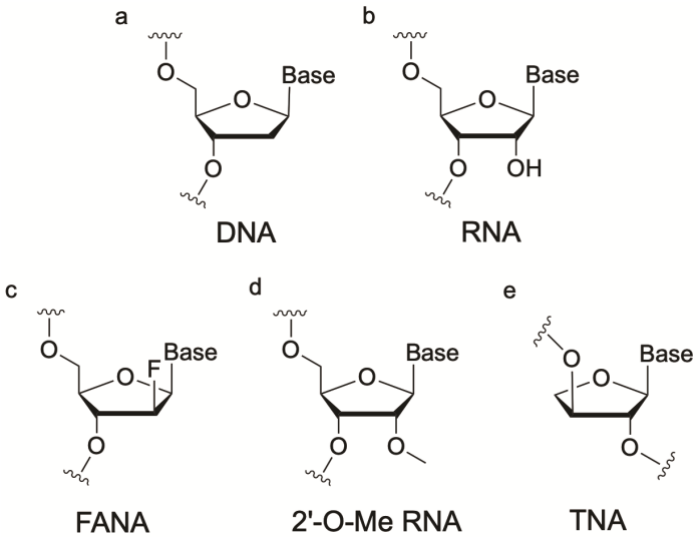

Figure 1.2. Chemical structures of common XNAs.

Recent work in the Heemstra lab used another nuclease stable approach with threose-nucleic acid, TNA, to develop a fully TNA aptamer.[31] TNA differs from DNA in the backbone, which is based on threose, rather than furanose. TNA has 3' to 2' connectivity, compared to DNA or RNA 5' to 3' connectivity and has a backbone connectivity that is one carbon atom shorter than DNA or RNA.[32,33] Despite these structural differences, TNA can still hybridize to DNA and RNA through Watson-Crick-Franklin base pairing, be reverse transcribed, and is nuclease resistant.[34,35] My first project set out to develop a nuclease resistant biosensor using a TNA aptamer.

Small molecule Sequestration with virus-like particles and nucleic acid aptamers

While detecting small molecules is important, there remains a critical need for an adaptable system that could sequester small molecules. An ideal sequestration system would have a high affinity reagent to capture the target molecule, have a container to enclose sequestered small molecules, and could function in multiple biological environments. To achieve this, we developed a system that encapsulates aptamers inside virus-like particle nanocontainers.

This sequestration system encapsulating nucleic acid aptamers inside a nanocontainer has two significant benefits. First, encapsulation will prevent nuclease interference, which addresses the main limitation of using aptamers in biological environments. Second, a nanocontainer coupled with aptamers will isolate and retain small molecules within the container to prevent interaction with the surrounding environment. We hypothesized that Virus-Like Particles (VLPs) could be used as nanocontainers in a sequestration system due to the hollow internal cavity which would allow aptamer to be attached, and small molecules to be encapsulated.

VLPs are biologically-derived hollow protein nanoparticles without viral genetic material. The key advantage of incorporating VLPs is the selective permeability of outer membrane, which will allow diffusion of a small target molecule, but exclude larger nucleases which protects the integrity of the inner nucleic acid aptamer.[36] VLPs are made up of a multimeric protein that can be easily expressed in high yields from bacterial cell culture and assembled *in vitro*.[37–39] Both of these structural VLP properties enable easy, selective aptamer conjugation onto the VLP interior surface.[40] The non-infectious properties of VLPs are also highly valuable as they will allow this sequestration system to be applied to both environmental or biological applications.[41]

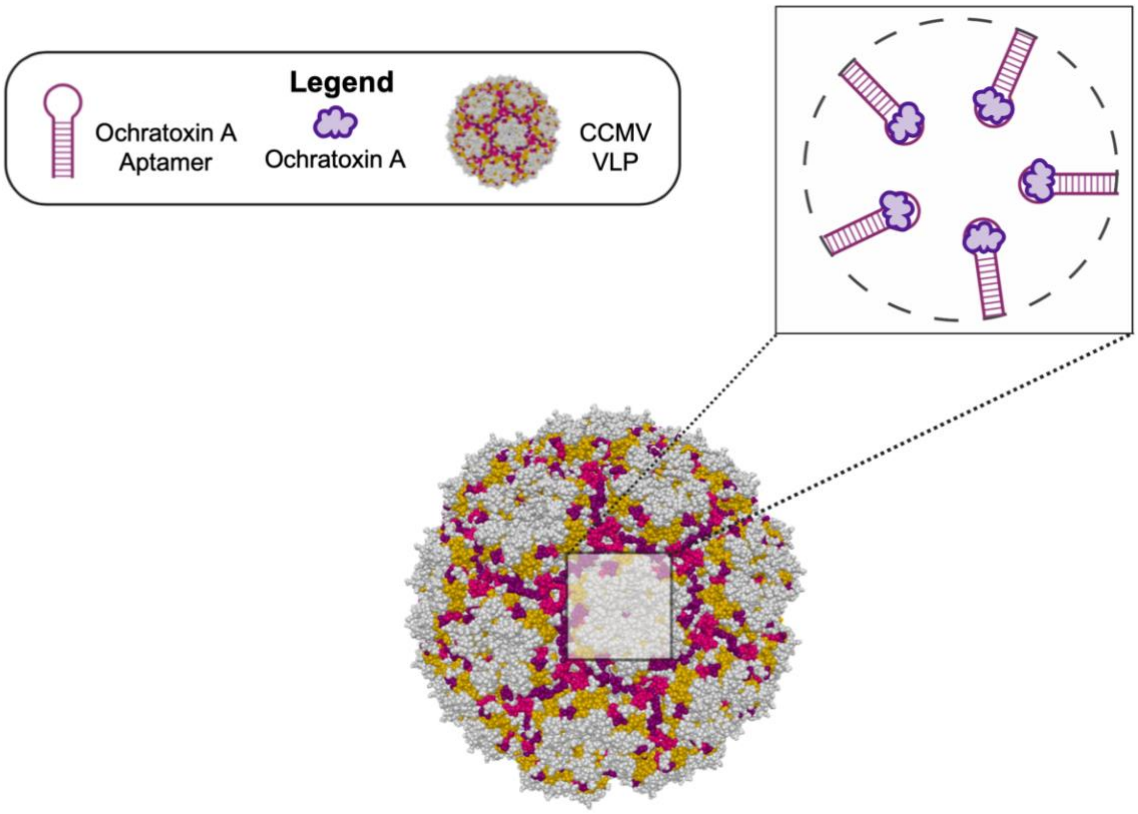

Figure 1.3. Nucleic acid aptamers conjugated to the internal cavity of virus-like particles to sequester small molecule toxins.

On their own, both aptamers and VLPs have limitations but, in combination they are a resistant and flexible sequestration system. For this project, aptamers will be conjugated to the internal cavity of the VLP and will bind and retain the target molecule within the nanocontainer (Figure 1.3). The porous VLP structure will allow small molecules to enter, but will exclude nucleases and proteases, providing biostability.[36] We hypothesize that this system will concentrate the target inside the nanocontainer which will allow for long-term capture and sequestration.

Ochratoxin as a Model System

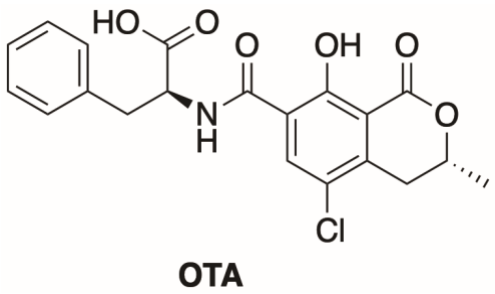

Figure 1.4. Chemical structure of Ochratoxin A.

We will be developing both the detection and sequestration systems for ochratoxin A (OTA), a small molecule toxin. OTA a mycotoxin that is produced by *Aspergillus ochraceus, Penicillium verrucosum, Aspergillus niger,* and *Aspergillus carbonarius*.[42] It is found most commonly in agricultural materials such as grains, wine, and coffee.[43] If ingested in large quantities, OTA can induce intense bouts of sweating, chest pain, and shortness of breath because of its carcinogenic, neurotoxic, and nephrotoxic effects.[44,45] OTA was chosen as our target molecule because it is easy to obtain, relatively safe to work with, and represents a large class of small molecules common in biology that have variable levels of toxicity.

Chapter 2: Small molecule detection with TNA based biosensor

Previous work in our lab used SELEX to select for a TNA aptamer capable of binding OTA with high affinity (K_D value of 71 ± 8 nM) (Figure 2.1).[31] Compared to a DNA aptamer, this TNA aptamer was shown to have superior nuclease stability following seven days incubation in 50% human blood serum.[31,46] This property of TNA overcomes a major limitation of DNA and RNA aptamers and provides stability in a nuclease-rich biological conditions and cellular environments.[34,35] After confirming that the TNA aptamer could perform in harsh conditions, we hypothesized that a TNA-based biosensor design could outperform standard DNA and RNA aptamers.

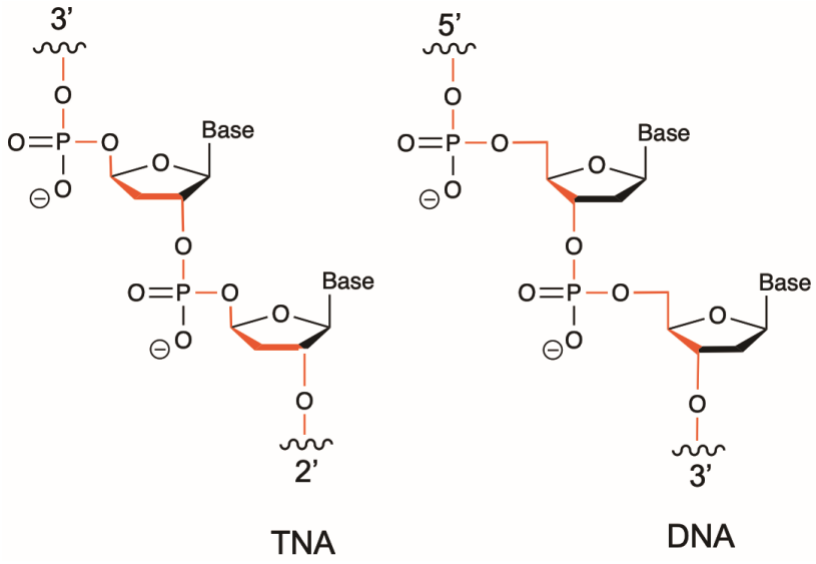

Figure 2.1. Chemical structures of TNA and DNA polymers. TNA has a 3' to 2' connectivity, DNA has a 5' to 3' connectivity.

As described above aptamers have been used in biosensors but are limited in their biological stability because of nuclease degradation.[26] Of the various types of biosensors, aptamers are uniquely suited to structure switching biosensors with a fluorescence-based detection.[47,48] Aptamers create excellent structure switching biosensors because they reliably form DNA-DNA duplexes with a specific complementary sequence and significantly change conformation when a

target molecule is introduced to the system.[47] The conformational change can be easily tracked using a fluorophore and a quencher on either strand. As seen in Figure 2.2, when the fluorophore-labeled aptamer is bound to the complementary strand functionalized with the quencher, the fluorophore and quencher will be in a close proximity suppressing the fluorescence output of the system. When the target molecule is introduced to the system, the aptamer will release the quenching strand and bind to the target molecule which increases fluorescence. The goal of this project was to develop a structure switching biosensor with the previously selected TNA aptamer to detect Ochratoxin A. The architecture of a structure switching biosensor includes the fluorescently labeled (FAM) TNA aptamer and a black hole quencher (BHQ) labeled complementary strand.

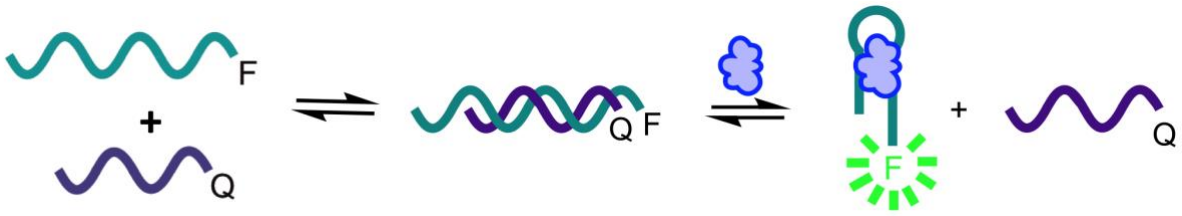

Figure 2.2. Structure switching biosensor architecture development using FAM labeled aptamer and BHQ1 labeled complementary sequence. When the target molecule is introduced to the system, it will displace the complementary strand, restoring fluorescence.

The first step of developing this structure switching biosensor was to design DNA displacement strands complimentary to the TNA aptamer sequence. We estimated that the sequence would need at least four nucleotides in the stem region of the TNA aptamer to effectively disrupt binding. Previous work in our lab has shown the optimal displacement strand length to be approximately 9-10 nucleotides (nt) long which creates a stable duplex at equilibrium. Therefore, we designed four initial complementary strands (Table 2.1) that ranged from 9-12 nt. Each of the complementary strands started in the stem region of the aptamer to facilitate hybridization of the displacement strand to the aptamer sequence. To enable fluorescence monitoring, we placed

FAM and black hole quencher (BHQ) near each other in a hybridized state with FAM at the 3' end of the TNA aptamer, and the black hole quencher (BHQ) at the 3' end of the complementary strand

A04T.2	3′-/FAM/AATAGGGTAAAAAAAAAAAGTTGGTCCTATG – 2′
AQ9	3′-/BHQ/TTATCCCAT – 5′
AQ10	3′-/BHQ/TTATCCCATT – 5′
AQ11	3′-/BHQ/TTATCCCATTT – 5′
AQ12	3′-/BHQ/TTATCCCATTTT – 5′

Table 2.1. Sequences of the A04T.2 TNA aptamer and complementary DNA sequences, ranging from 9-12 nucleotides.

The second step was to analyze quenching of the fluorescence signal at varying concentrations of the BHQ-labeled DNA. Each complementary strand quenching was tested in a 1:1 ratio of complementary strand and aptamer with concentrations ranging from 30-1000 nM for each sequence (Figure 2.3). As expected, these data confirmed that all four complementary strands were capable of quenching and increasing the concentrations of the aptamer and complementary strand increased quenching.

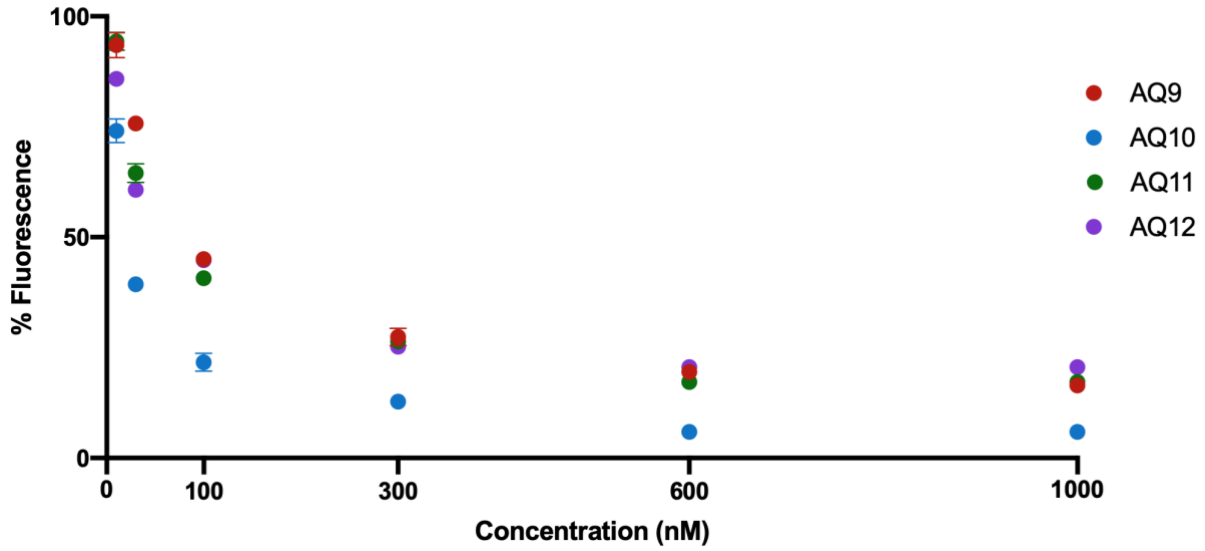

Figure 2.3. Fluorescence quenching at a 1:1 ratio of TNA A04T.2 aptamer and complimentary quenching strand.

To develop a sensitive assay, the biosensor must have both high levels of quenching and the ability to restore fluorescence in the presence of the target molecule. However, our results showed the highest level of quenching corresponded with a very high biosensor concentration (1000 nM) that shifted the equilibrium in favor of the hybridized system which prevented interactions with the target molecule. To overcome this issue subsequent experiments were carried out at concentrations of 60-100 nM.

Next, we assessed the biosensor sensitivity with varying ratios of aptamer and complementary strand. A 1:1, 1:2 and 1:3 of aptamer to complementary strand ratios were used (Figure 2.4). These experiments showed a modest increase in quenching as the ratio of aptamer to complementary strand increased. These nominal results were relatively similar and the 1:1 ratio of biosensor to complementary strand (AQ9) was used in future experiments.

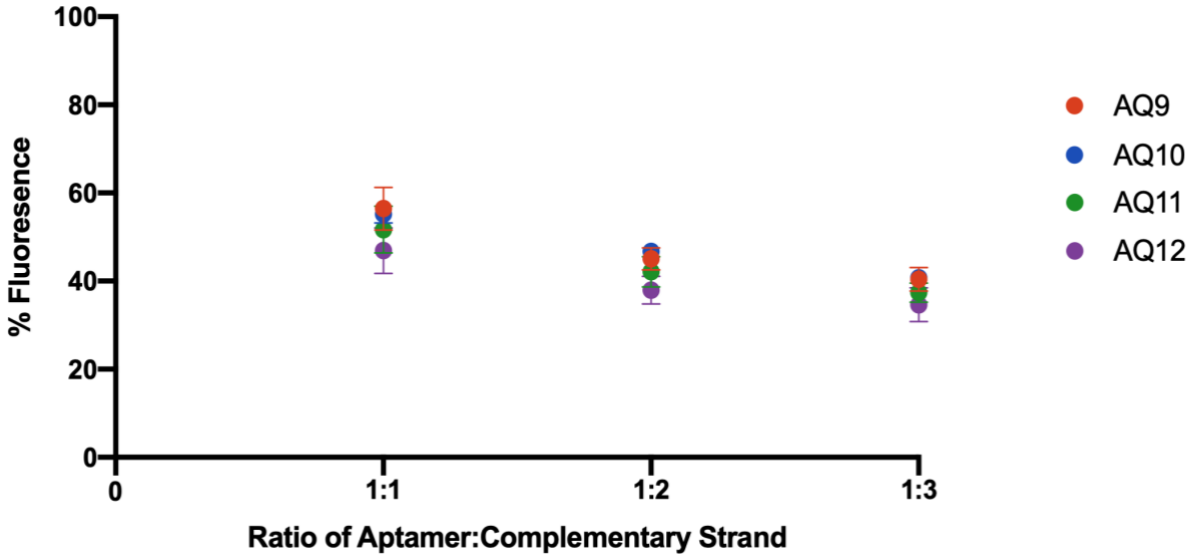

Figure 2.4. Fluorescence quenching of AQ9, AQ10, AQ11 and AQ12 with a constant TNA A04T.2 aptamer concentration (60 nM) with various ratios of complementary strand.

To further optimize the system, the third step was to test different binding locations of the complementary strand. The nine-nucleotide complementary strand was shifted by one nucleotide along the aptamer strand to create four additional complementary strand sequences (Table 2.2).

A04T.2	3′-/FAM/AATAGGGTAAAAAAAAAAAGTTGGTCCTATG – 2′
AQ9	3′-/BHQ/TTATCCCAT – 5′
AQ9.1	3′-/BHQ/TATCCCATT – 5′
AQ9.2	3′-/BHQ/ATCCCATTT – 5′
AQ9.3	3′-/BHQ/TCCCATTTT – 5′
AQ9.4	3′-/BHQ/CCCATTTTT – 5′

Table 2.2. Sequences of the A04T.2 TNA aptamer and four new complementary sequences, AQ9.1-AQ9.4. All new complementary sequences are nine nucleotides long and were designed by shifting along the A04T.2 aptamer sequence.

Each of these additional strands were able to quench the FAM-labeled A04T.2 (Figure 2.5). To maintain equilibrium, we decided to move forward with 60-100 nM biosensor concentration.

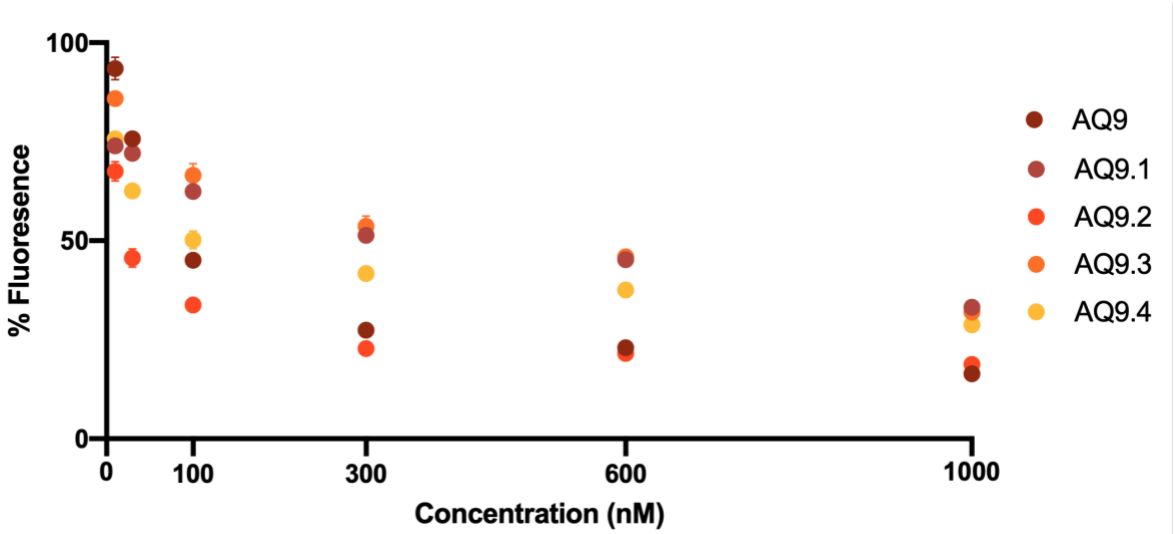

Figure 2.5. Fluorescence quenching at a 1:1 ratio of TNA A04T.2 aptamer and complimentary quenching strand.

We then assessed the biosensor sensitivity with the four new 9 nt complementary strands with varying ratios of aptamer. A 1:1, 1:2 and 1:3 of aptamer to complementary strand ratios were used (Figure 2.6). These experiments showed a modest increase in quenching as the ratio of aptamer to complementary strand increased.

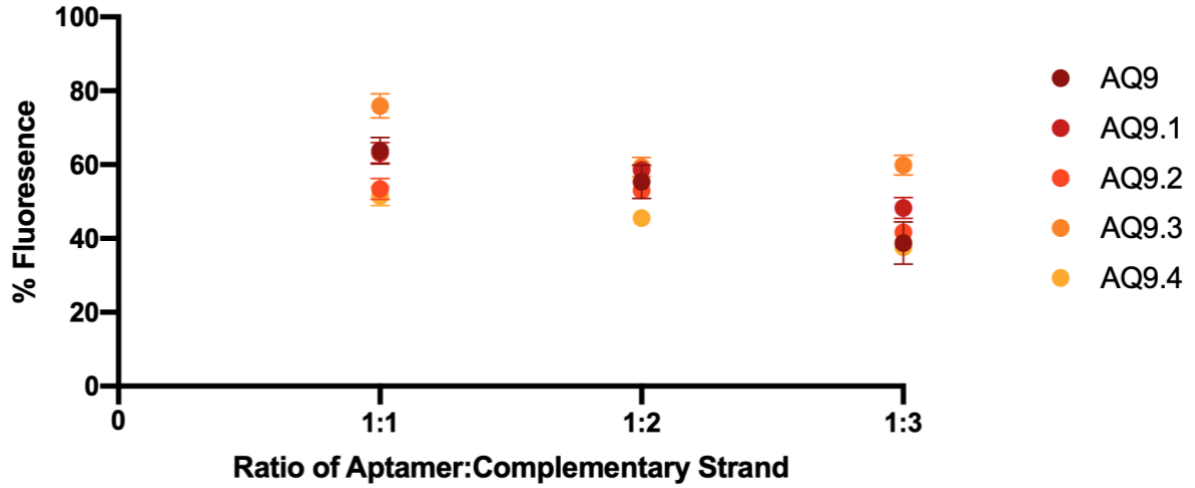

Figure 2.6. Fluorescence quenching of AQ9, AQ9.1, AQ9.2, AQ9.3, and AQ9.4 at various ratios of TNA A04T.2 aptamer to complementary strand.

After quenching was measured, 50 μM of OTA was added to the system and percent displacement was calculated (Equation 1) to validate the biosensor system (Figure 2.7).[49] Where F is the measured fluorescence of the sample, F_0 is the fluorescence intensity of the quenched biosensor and F_{max} is the fluorescence intensity of the unquenched sensor.

$$Percent\ Displacement = \frac{F - F_0}{F_{max} - F_0} \qquad \text{Equation1}$$

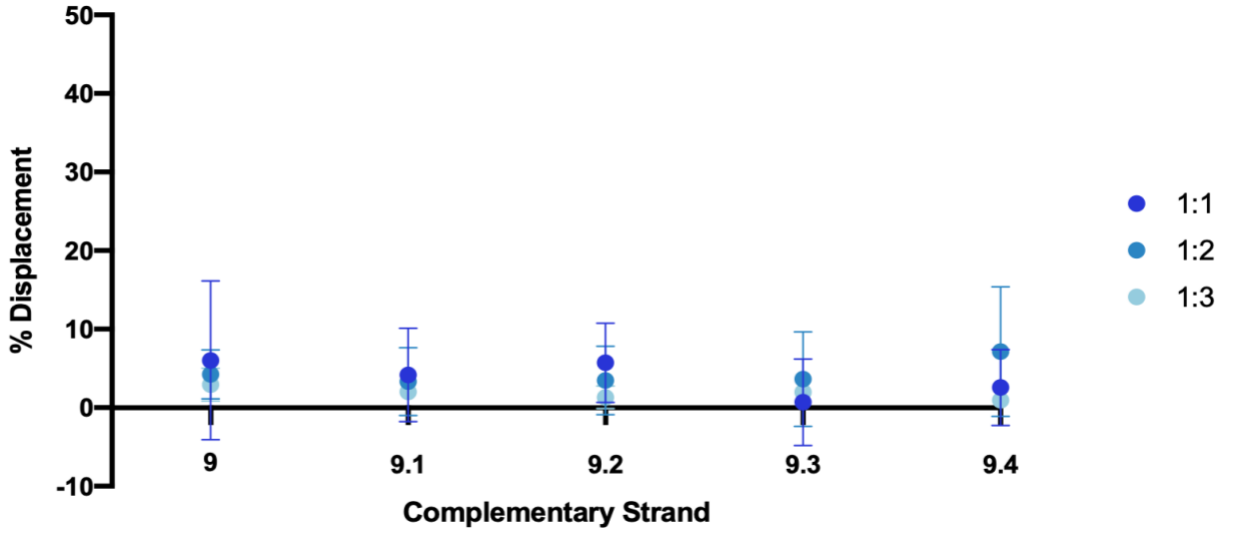

Figure 2.7. The percent displacement was calculated from 60 nM A04T.2 with varying ratios of AQ9-AQ9.4 complementary strand, upon the addition of 50 μM of OTA.

Ultimately, we did not see any displacement of the complementary strand with the addition of OTA, but we were unsure why. Since little is known about TNA duplex stability, we tested the stability of the TNA:DNA duplex over time. To do this we used a 100 nM biosensor concentration, at a 1:1 ratio with AQ9 and found that the percent fluorescence more than doubled after 45 minutes at room temperature (Figure 2.8).

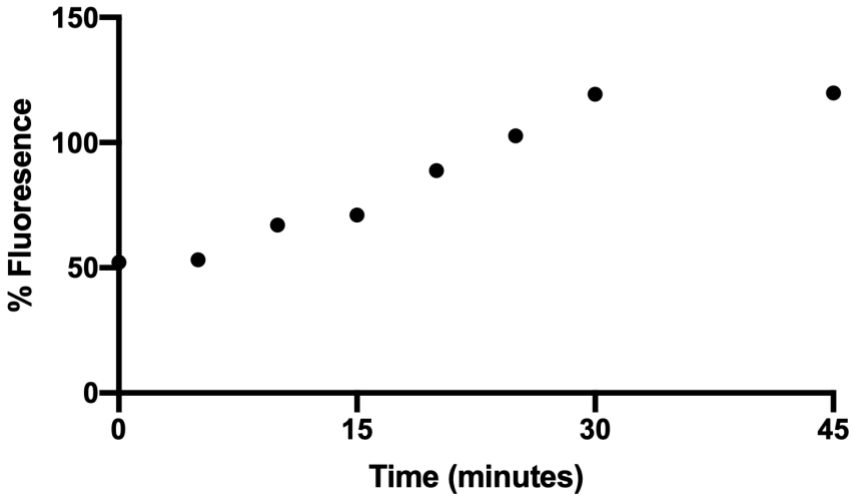

Figure 2.8. Fluorescence of the A04T.2:AQ9 biosensor duplex (100 nM, 1:2 ratio) doubles after sitting at room temperature for 45 minutes.

Conclusions and Future Work

The work reported here reflects our current progress in the effort to develop a TNA-based biosensor for the detection of Ochratoxin A. We have designed and optimized complementary sequences, and confirmed dose dependent fluorescence quenching. Future work on this project could be done to explore the kinetics of TNA:DNA duplexes, and determine stable conditions for future biosensor experiments. Once the system conditions have been optimized, future work on this project could be done to determine where OTA is binding within the aptamer sequence by further shifting the complementary strand along the loop. This test could provide more insight on the biological interaction and allow for further optimization. We chose to first work with the A04T.2 TNA aptamer due to its stronger binding affinity, however, one of the other TNA aptamer sequences (B29) could also be tested.[31] A TNA based biosensor capable of detecting small molecule toxins, could close the gap in biological applications where aptamer-based biosensors are commonly limited due to nuclease degradation.

Chapter 2: Methods

Buffer Preparation

Reagents were purchased from Sigma-Aldrich, Thermo Fisher, Millipore Sigma, and Fisher Scientific, or EMD Millipore and used as received. Buffers were pH adjusted with Thermo Fisher pH meter and filtered through 0.2 μm filters prior to use.

TNA and DNA sequences

TNA phosphoramidites were synthesized by unpublished methods developed in our lab for solid phase synthesis of TNA sequences. All DNA sequences were purchased from the University of Utah DNA/Peptide Synthesis Core Facility. TNA aptamer and DNA complementary strands were synthesized by the University of Utah DNA/Peptide Synthesis Core Facility at a 1 μmol scale (Table 2.3). The TNA aptamer strand was FAM labeled on the 3' end, and all DNA complementary strands were labeled with BHQ1 on 3' end.

Sequence Name	Sequence
A04T.2 Aptamer	3'-/FAM/AATAGGGTAAAAAAAAAAAGTTGGTCCTATG-2'
AQ9	5'-TACCCTATT/BHQ1/-3'
AQ10	5'-TTACCCTATT/BHQ1/-3'
AQ11	5'-TTTACCCTATT/BHQ1/-3'
AQ12	5'-TTTTACCCTATT/BHQ1/-3'
AQ9.1	5'-TTACCCTAT/BHQ1/-3'
AQ9.2	5'-TTTACCCTA/BHQ1/-3'
AQ9.3	5'-TTTTACCCT/BHQ1/-3'
AQ9.4	5'-TTTTTACCC/BHQ1/-3'

Table 2.3. All TNA and DNA sequences used for the development of a small molecule detection with a TNA based biosensor.

TNA and DNA purification

Both TNA and DNA sequences were purified on 10% PAGE gel containing 8 M urea. The gel was run for 45 min at 275 volts, and was imaged using an UltraBright UV Transilluminator. The desired band was removed and incubated in crush and soak buffer (300 mM ammonium acetate, 1 mM EDTA, pH 8) at -80°C for 15 minutes then at 90°C for 2 hours. The isolated sequence was then separated from excess gel pieces and buffer exchanged into water using Amicon Ultra-0.5 Centrifugal Unit with Ultracel 10 membrane (EMD Millipore). Samples were quantified using Nanodrop and stored at -20°C until further use.

Fluorescent Biosensor Preparation

Biosensor experiments were prepared in TNA binding buffer (10mM Tris-HCl, 120 mM NaCl, 5 mM KCl, 1 mM $CaCl_2$, pH 8.4) and calculated to have a final volume of 100 μL. Prior to any fluorescence readings, biosensor samples were first heated to 90°C for 5 min, cooled at 4°C for 10 min, then incubated at 25°C for 30 min to allow for aptamer-complementary strand annealing.

Biosensor Percent Displacement Calculations

Following the 30 min incubation, samples were then transferred to a Corning 96-well flat bottom clean polystyrene plate. The samples were scanned for fluorescence intensity on a Biotek Synergy 2 multimode plate reader using excitation/emission wavelengths of 494/525 nm. All experimental samples were run along with two controls: an unquenched sensor (contained the TNA aptamer strand) and a quenched sensor (containing the FAM-labeled TNA aptamer and BHQ-labeled complementary strand). Using these values, the % Fluorescence values were standardized using a control solution containing only the FAM-labeled TNA aptamer sequence. The % displacement was calculated using Equation 1.

$$Percent\ Displacement = \frac{F - F_0}{F_{max} - F_0}$$

Where F is the measured fluorescence of the sample, F_0 is the fluorescence intensity of the quenched biosensor and F_{max} is the fluorescence intensity of the unquenched sensor.

Chapter 3: Small molecule Sequestration with virus-like particles and nucleic acid aptamers

To create a sequestration system, we combined the previously reported OTA DNA aptamer, A08m,[46] and cowpea chlorotic mottle virus (CCMV) VLP (Figure 1). CCMV is a single-stranded RNA, plant-based virus, and a member of the *Bromovirus* genus.[39] It has an outer diameter of 28 nm, inner diameter of 18 nm, and is made up of 180 coat proteins.[50] The assembled VLP has 2 nm pores on the surface which would allow OTA (<1 nm) to enter, and internally conjugated aptamers will retain OTA inside the CCMV cavity.[51]

a

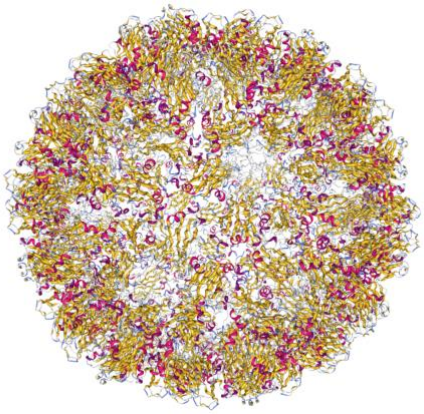

b

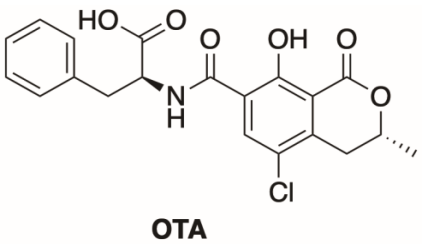

c

A08m: NH_2/GGCAGTGTGGGCGAATCTATGCGTACCGTTCGATATCGTG/FAM

Figure 3.1. Relevant structures (a) cowpea chlorotic mottle virus assembled VLP (b) previously reported ochratoxin A DNA aptamer sequence (c) Ochratoxin A chemical structure.

The native CCMV protein does not have many sites for a covalent internal attachment of DNA aptamers. Therefore, we designed a mutant protein with a lysine to cysteine point mutation in the internal structure of the VLP. Cysteine was selected because it is the most common amino acid used for maleimide attachments.[52] Based on the reported crystal structure of CCMV VLP (PDB

1ZA7)[53] there are three possible internal lysines located at amino acid positions 45, 87 and 143. Lys-45 is located on an N-terminal region that has been shown to contribute to the VLP tertiary structure and if mutated this could interfere with VLP assembly. Lys-87 and lys-143 are near each other in the core of the coat protein, lys-87 is facing into the VLP pores which if altered may interfere with entering particles. However, lys-143 points towards the interior of the coat protein, which is an ideal location that will not interfere with entering particles or change the conformational shape of the CCMV protein (Figure 3.2).

Native CCMV gene
MSTVGTGKLTRAQRRAAARKNKRNTRVVQPVIVEPIASGQGKAIKAWTGYSVSKWTASCAAAEAKVTSAITISLPNEL
SSERNKQLKVGRVLLWLGLLPSVSGTVKSCVTETQTTAAASFQVALAVADNSKDVVAAMYPEAFKGITLEQLKADLTIY
LYSSAALTEGDVIVHLEVEHVRPTFDDSFTPVY

Mutated CCMV gene
MSTVGTGKLTRAQRRAAARKNKRNTRVVQPVIVEPIASGQGKAIKAWTGYSVSKWTASCAAAEAKVTSAITISLPNEL
SSERNKQLKVGRVLLWLGLLPSVSGTVKSCVTETQTTAAASFQVALAVADNSKDVVAAMYPEAFKGITLEQLCADLTIY
LYSSAALTEGDVIVHLEVEHVRPTFDDSFTPVY

Figure 3.2. Native and mutated CCMV gene sequence with the chosen lysine to cysteine amino acid mutation highlighted.

The CCMV gene was mutated and the change was confirmed by Sanger sequencing. The native and mutant CCMV protein was expressed in a pET28a vector, purified by nickel his-tag chromatography and verified by SDS-PAGE (Figure 3.3).

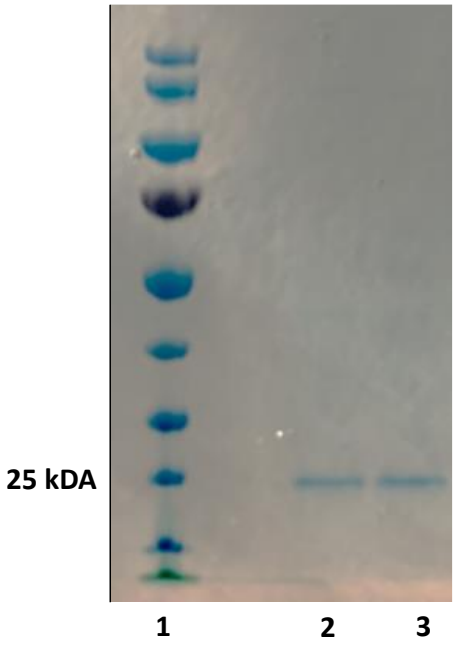

Figure 3.3. Purified native and mutant CCMV protein run on a NuPAGE 4-12% Bis-Tris gel. Lane 1: PageRuler Prestained protein ladder, 10-180 kDa. Lane 2: Purified native CCMV protein at 26 kDa. Lane 3: Purified mutant CCMV protein at 26 kDa.

The OTA aptamer (13 kDa) was conjugated to the mutant protein (26 kDa) through a maleimide linker with 65% protein labeling and was confirmed by SDS-PAGE (40 kDa) (Figure 3.4). The mutant protein-aptamer conjugation was verified by size exclusion chromatography, and conjugation was confirmed by an overlapping nucleic acid (280 nm) and FAM (495 nm) elution at 33.5 minutes (Figure 3.4).

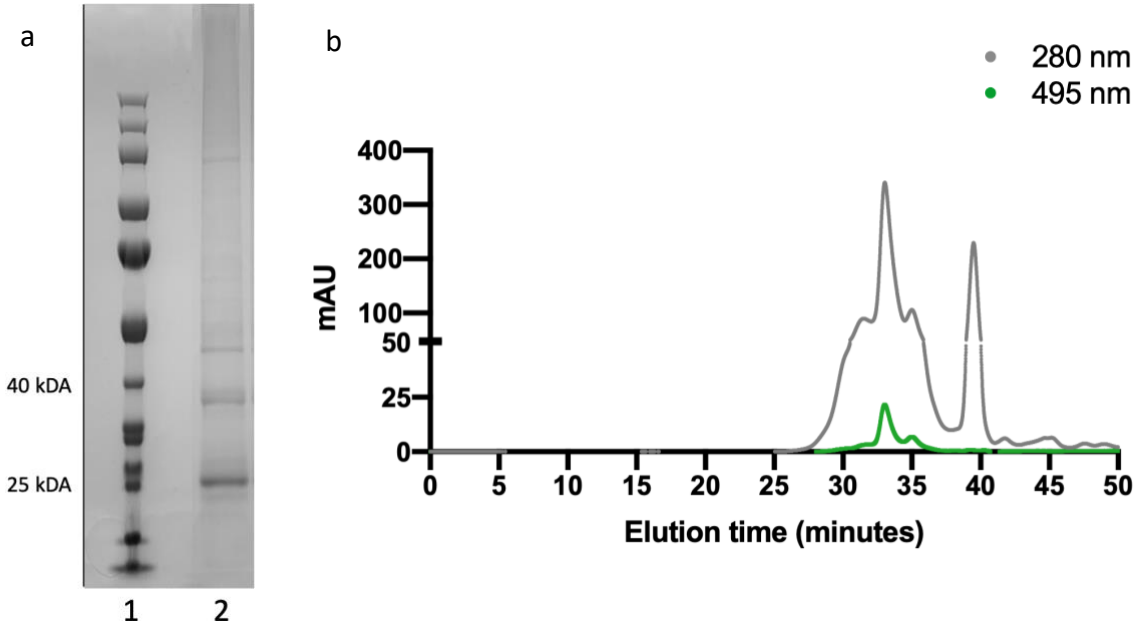

Figure 3.4. (a) Mutant protein-aptamer conjugation reaction run on NuPAGE 4-12% Bis-Tris gel. Lane 1: PageRuler Prestained protein ladder, 10-180 kDa. Lane 2: Mutant protein-aptamer conjugation. (b) Size-exclusion chromatography trace of mutant protein-aptamer conjugation on Superose 6 increase 10/300 GL column.

After confirmation of the mutant CCMV aptamer conjugation was verified, the assembly properties of the VLP nanocontainer were examined. CCMV VLP nanocontainers undergo pH-dependent self-assembly and disassembly.[54] Once native CCMV protein expression had been purified and confirmed, native VLP assembly was tested by dialyzing 50 μM CCMV native protein overnight in assembly buffer and 28 nm assemblies were confirmed by transmission electron microscopy (Figure 3.5).

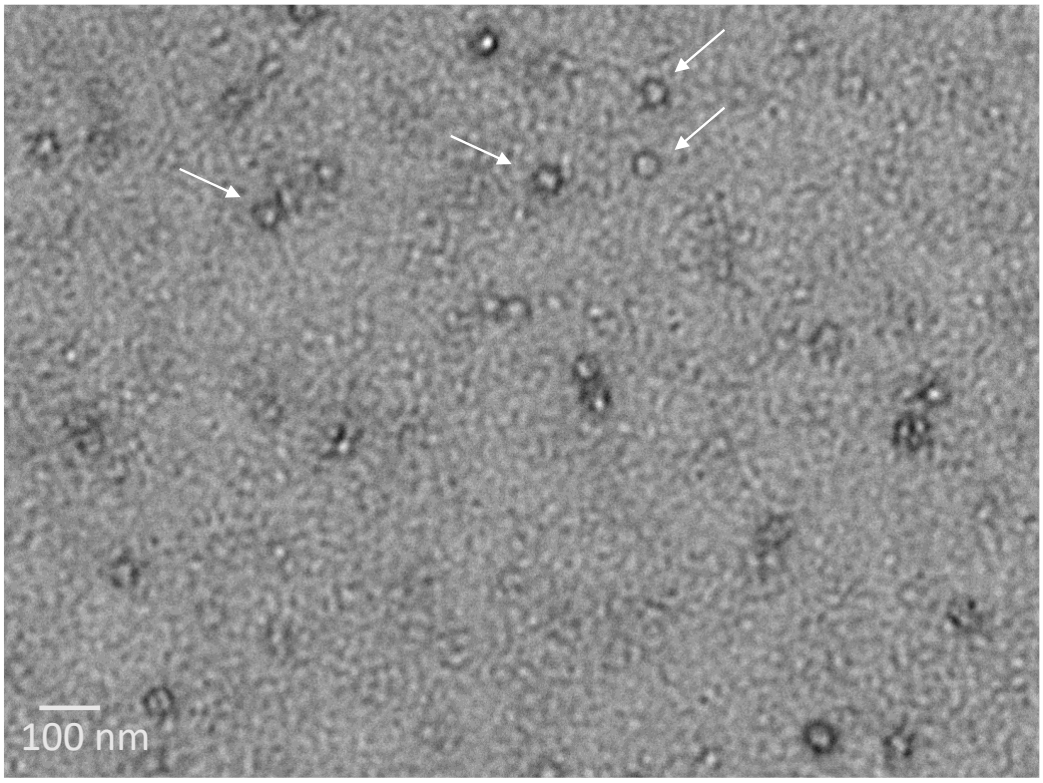

Figure 3.5. TEM of native VLP CCMV assemblies, 28 nm in diameter. Assembled in 1 M NaCl, 50 mM NaOAc, 1 mM NaN_3, pH 5 in 12 - 14 kDa dialysis tubes, overnight at 4°C.

The next step was to assemble a VLP with internally conjugated OTA specific DNA-aptamers. In the process of purifying excess aptamer from protein conjugated aptamer we discovered that the OTA aptamer could conjugate with both the mutant and wild-type CCMV protein (Figure 3.6). This was an unexpected result because only the mutant CCMV protein should have the necessary active cystines that could conjugate with the OTA aptamers.[55]

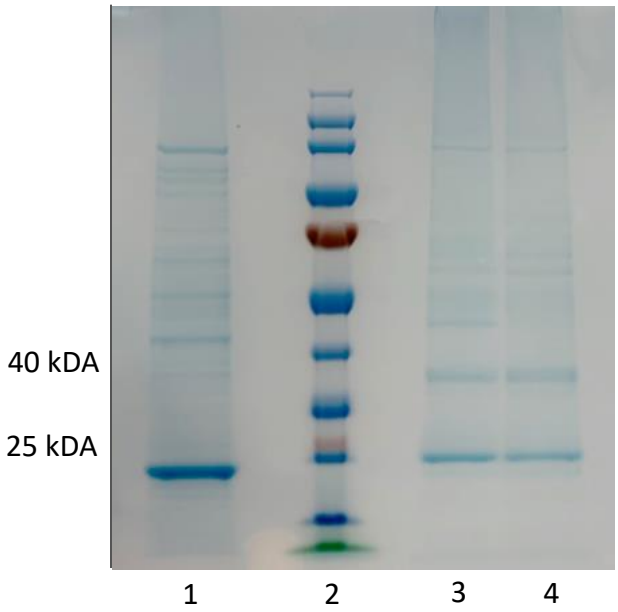

Figure 3.6. CCMV native and mutant protein-aptamer conjugation reaction run on NuPAGE 4-12% Bis-Tris gel. Lane 1: Purified mutant protein. Lane 2: PageRuler Prestained protein ladder, 10-180 kDa. Lane 3: Mutant CCMV protein-aptamer conjugation. Lane 4: Native CCMV protein aptamer conjugation.

To troubleshoot this unexpected conjugation, we examined the CCMV sequences by sanger sequencing to confirm the native and mutated sequences. Sanger sequencing revealed a N-terminal addition of 34 amino acids was inserted which contained an additional cysteine, an HRV cleaving site, and other unexpected amino acids (Figure 3.7).

Native CCMV gene
MSTVGTGKLTRAQRRAAARKNKRNTRVVQPVIVEPIASGQGKAIKAWTGYSVSKWTASCAAA
EAKVTSAITISLPNELSSERNKQLKVGRVLLWLGLLPSVSGTVKSCVTETQTTAAASFQVALAVA
DNSKDVVAAMYPEAFKGITLEQLKADLTIYLYSSAALTEGDVIVHLEVEHVRPTFDDSFTPVY

Native CCMV gene – N term insertion
MGHHHHHHHHHLCSGHIDDDDNHTSLEVLFQGPHMSTVGTGKLTRAQRRAAARKNKRNTRV
VQPVIVEPIASGQGKAIKAWTGYSVSKWTASCAAAEAKVTSAITISLPNELSSERNKQLKVGRVL
LWLGLLPSVSGTVKSCVTETQTTAAASFQVALAVADNSKDVVAAMYPEAFKGITLEQLKADLTI
YLYSSAALTEGDVIVHLEVEHVRPTFDDSFTPVY

Figure 3.7. Sanger sequencing results showed a 34 aa N terminal insertion.

With the discovery of incorrect amino acid sequences within the wild-type and mutant we needed to determine where the OTA aptamer was conjugating on the mutant CCMV protein. We found that 84% of the aptamer was conjugated to an additional N-terminal cystine, which we discovered by cleaving the conjugated CCMV protein at the HRV site (Figure 3.8)

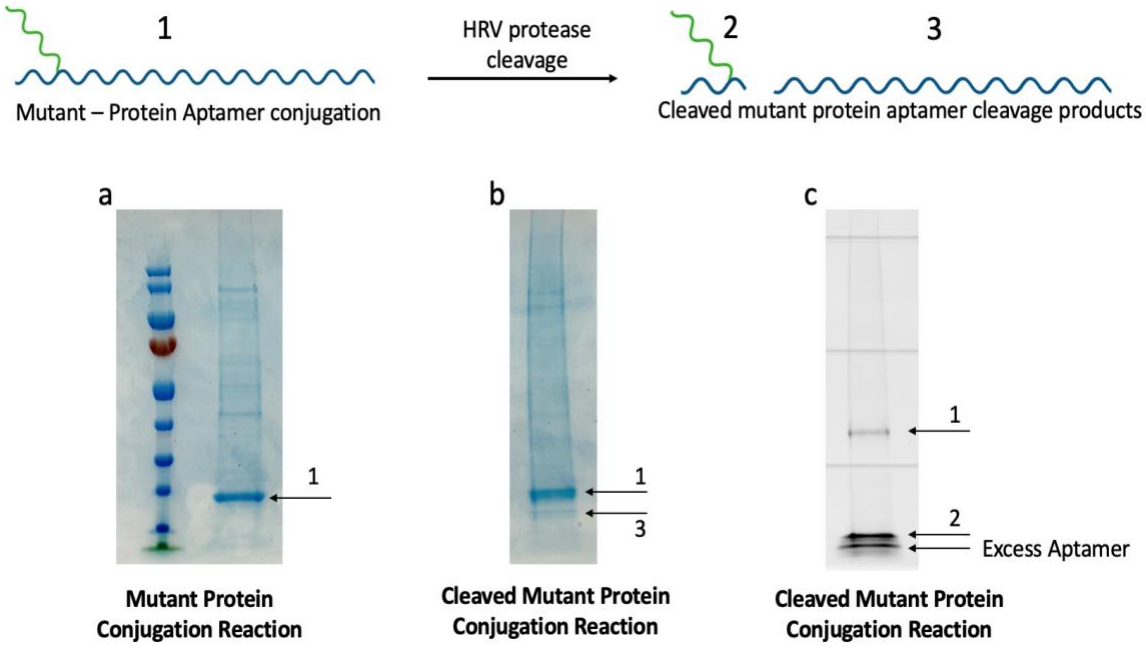

Figure 3.8. CCMV mutant protein HRV cleavage reaction run on NuPAGE 4-12% Bis-Tris gel. (a) Lane 1. PageRuler Prestained protein ladder, 10-180 kDa. Lane 2. Purified mutant protein at 26 kDa. (b) Mutant protein after HRV cleavage reaction. Run on NuPAGE 4-12% Bis-Tris gel. (c) Mutant protein after HRV cleavage reaction. Run on NuPAGE 4-12% Bis-Tris gel, imaged with FITC filter.

Conclusions and future directions

The work reported here reflects our current progress in the effort to develop a new small-molecule sequestration method to capture Ochratoxin A. We have expressed and purified native and mutated CCMV protein, and confirmed the protein size at 26 kDa by SDS-PAGE and size

exclusion chromatography. Native protein VLP assembly was tested, and TEM results confirm the presence of 28 nm virus-like particles. The OTA DNA aptamer was conjugated to the CCMV protein through a maleimide linker and characterized by SDS-PAGE and size exclusion chromatography. While this HRV cleavage site insertion was added as an error, we believe this could be a potentially good option moving forward for aptamer labeling. The HRV cleavage site insertion did not affect WT VLP assembly, and we saw very high levels of aptamer conjugation. Also, the added N-term cysteine is located on the interior of the VLP, and should be able to conjugate OTA DNA aptamers within the container without disrupting assembly.

Chapter 3 Methods

Buffer Preparation

Reagents were purchased from Sigma-Aldrich, Thermo Fisher, Millipore Sigma, and Fisher Scientific, or EMD Millipore and used as received. Buffers were pH adjusted with Thermo Fisher pH meter and filtered through 0.2 µm filters prior to use.

DNA sequences and modifiers.

All DNA aptamer sequences were purchased from the University of Utah DNA/Peptide Synthesis Core Facility and purified on a 10% PAGE gel containing 8 M urea. The gel was run for 40 min at 275 volts, and was imaged using an UltraBright UV Transilluminator. The desired band was removed and incubated in crush and soak buffer (300 mM ammonium acetate, 1 mM EDTA, pH 8) at -80°C for 15 minutes then at 90°C for 2 hours. The isolated sequence was then separated from excess gel pieces and buffer exchanged into water using Amicon Ultra-0.5 Centrifugal Unit with Ultracel 10 membrane (EMD Millipore). Samples were quantified using Nanodrop and stored at -20°C until further use.

CCMV mutation

The Emory Integrated Genomics core at Emory University preformed the lysine 143 to a cysteine point mutation and inserted both the CCMV native and mutated gene into a pET28a vector. The vector was amplified in BL21 (DE3) E. Coli and plasmid DNA was recovered using a Qiagen miniprep kit. These DNA plasmids were then sequenced the Emory Integrated Genomics core at Emory University and the sequences were confirmed.

CCMV protein expression

CCMV native and mutant protein was expressed in Rosetta-gami 2 (DE3) E. Coli cells. Plasmid, pET28, was transformed into competent cells and plated on LB agar plates containing 50 μg/mL kanamycin. Colonies were picked and grown in 6 mL LB overnight cultures. They were then transferred into 1 L of LB containing 50 μg/mL kanamycin. Expression was induced at OD600 of 0.6 by adding IPTG to 1 mM final concentration. Cultures were allowed to grow at 37 °C for 4 h in a shaking incubator at 250 rpm. The native and mutant CCMV protein was then pelleted and frozen at -80°C, followed by lysis with BPER (Bacterial Protein Extraction Reagent by Thermo Fisher).

CCMV protein purification

Protein was purified using Ni-NTA agarose beads (Thermo Fisher). 2 mL of Ni-NTA resin was added and equilibrated with equilibration buffer (50mM sodium phosphate, 300mM sodium chloride, pH 7.4). Protein samples were mixed with an equal volume of equilibration buffer and added to the resin bed. Protein extract and resin was mixed on end-over-end rotator for 30 minutes, centrifuged for 2 min at 700 x g. Resin was washed 4X with two resin-bed volumes of equilibration buffer. This protein – resin wash cycle was repeated 2X with B1, 4X with B2 (50mM sodium phosphate, 300mM sodium chloride, 10mM imidazole, pH 7.4), 3X with B3 (50mM sodium phosphate, 300mM sodium chloride, 25mM imidazole, pH 7.4), and 2X with B4 (50mM sodium phosphate, 300mM sodium chloride, 150mM imidazole, pH 7.4). The B3 supernatant containing purified CCMV native and mutant protein was concentrated and buffer exchanged into PBS using 30 kDa MWCO ultra centrifugal filters (Amicon). Protein purity was confirmed by SDS-PAGE (by Coomassie stain) and the concentration was determined using Micro BCA Protein Assay (Thermo Fisher).

SDS-PAGE and Imaging

CCMV protein and CCMV protein – aptamer samples were diluted to 10 μM with protein storage buffer (50 mM Tris, 500 mM NaCl, 10 mM $MgCl_2$, 1 mM EDTA, pH 7.2) and diluted with equal volume of RNA loading dye (2X) purchased from NEB. Samples were loaded onto NuPAGE 4-12% Bis-Tris protein gels, purchased from Thermo Fisher, and run for 60-80 min at 200 V. A 10-180 pre-stained protein ladder, purchased from Thermo Fisher, was run alongside each sample. The gels were first imaged on an Amersham Typhoon 5 laser scanner for aptamer fluorescence, then, protein size was imaged with Coomassie Blue stain.

Coomassie Blue Stain and Destain

After aptamer fluorescence was imaged, the gel was stained with Coomassie stain (1 g Coomassie Blue R 250 in 50% MeOH, 10% CH_3COOH, 40% H_2O). The gel was microwaved in coomassie stain for 2 min, then rotated at room temperature for 40 min. Gel was then destained (25% MeOH, 10% CH_3COOH, 65% H_2O) until background was clear.

CCMV aptamer protein labeling methods

The CCMV mutant protein – aptamer conjugation reactions were performed with Sulfo-SMCC maleimide linker (Thermo Scientific). First, 2 mg of sulfo-SMCC was dissolved in 200 μL of ultrapure H_2O, and vortexed to dissolve completely. The DNA Ochratoxin A aptamer (5' amine labeled) was added to the solution, along with 200 μL of SMCC buffer (100 mM NaH_2PO_4, 150 mM NaCl, pH 7.2). The sample was allowed to react for 2-4 hours at 4°C, then excess sulfo-SMCC crosslinker was removed with a Zeba desalting column (Thermo Fisher). CCMV protein was added and the reaction was allowed to react overnight, at 4°C. Aptamer conjugation was

analyzed and confirmed by SDS-PAGE gel electrophoresis, typhoon imaging, SEC HPLC and coomassie stain.

Size Exclusion Chromatography – High Performance Liquid Chromatography

A 100 μL sample of CCMV mutant – aptamer conjugated protein was separated in a Superdex 200 Increase 10/300 GL column (GE Healthcare Bio-Sciences) at 0.5 mL/minute with a running buffer consisting of 50 mM NaOAc, 500 mM NaCl, 10 mM $MgCl_2$. Absorbance was measured at 280 nm for protein and aptamer nucleic acid content, and 495 nm for the FAM labeled aptamer. The overlapping 280 nm and 495 nm peaks were collected, concentrated with 30 kDa MWCO ultra centrifugal filters (Amicon) and analyzed by SDS-PAGE gel electrophoresis and Coomassie Blue staining.

CCMV VLP Transmission Electron Microscopy

200 mesh Formvar/carbon-coated copper grids were first glow-discharged using a GloQube Plus Glow Discharge system. CCMV protein was dissolved in VLP assembly buffer (50 mM NaOAc, 500 mM NaCl, 10 mM $MgCl_2$, 1 mM EDTA, pH 5) and diluted to a concentration of 0.2 mg/mL, and 5 μL of sample was placed onto the grid. Samples were allowed to incubate for 15 min, and excess sample was blotted away with filter paper. Grids were allowed to dry for 5 min, then stained with 2% uranyl acetate for 15 sec, blotting away excess liquid and allowed to dry for 30 min before TEM analysis.

Refences

1. Penedo, J. C., Mulchandani, A., Derosa, M. C. & Ruscito, A. Small-Molecule Binding Aptamers: Selection Strategies, Characterization, and Applications. *Front. Chem.* **1**, 14 (2016).
2. Roemer, T., Davies, J., Giaever, G. & Nislow, C. Bugs, drugs and chemical genomics. *Nature Chemical Biology* **8**, 46–56 (2012).
3. Walsh, T. A. The emerging field of chemical genetics: potential applications for pesticide discovery. *Pest Manag. Sci.* **63**, 1165–1171 (2007).
4. Ney, Y., Nasim, M. J., Kharma, A., Youssef, L. A. & Jacob, C. Small molecule catalysts with therapeutic potential. *Molecules* **23**, (2018).
5. Mckeague, M. & Derosa, M. C. Challenges and Opportunities for Small Molecule Aptamer Development. *J. Nucleic Acids* **2012**, 20 (2012).
6. Ruscito, A. & DeRosa, M. C. Small-molecule binding aptamers: Selection strategies, characterization, and applications. *Frontiers in Chemistry* **4**, (2016).
7. Groff, K., Brown, J. & Clippinger, A. J. Modern affinity reagents: Recombinant antibodies and aptamers. *Biotechnology Advances* **33**, 1787–1798 (2015).
8. Chames, P., Van Regenmortel, M., Weiss, E. & Baty, D. Therapeutic antibodies: Successes, limitations and hopes for the future. *British Journal of Pharmacology* **157**, 220–233 (2009).
9. Ali, M. H., Elsherbiny, M. E. & Emara, M. Updates on aptamer research. *International Journal of Molecular Sciences* **20**, 2511 (2019).
10. Song, K. M., Lee, S. & Ban, C. Aptamers and their biological applications. *Sensors* **12**, 612–631 (2012).
11. Lakhin, A. V., Tarantul, V. Z. & Gening, L. V. Aptamers: Problems, solutions and prospects. *Acta Naturae* **5**, 34–43 (2013).
12. Ka Lok Hong & Letha J Sooter. Single-Stranded DNA Aptamers against Pathogens and

Toxins: Identification and Biosensing Applications. *Comput. Math. Methods Med.* **2015**, 2–4 (2015).

13. Dunn, M. R., Jimenez, R. M. & Chaput, J. C. Analysis of aptamer discovery and technology. *Nat. Rev. Chem.* **1**, 1–16 (2017).
14. Zichel, R., Chearwae, W., Pandey, G. S., Golding, B. & Sauna, Z. E. Aptamers as a sensitive tool to detect subtle modifications in therapeutic proteins. *PLoS One* **7**, (2012).
15. Ku, T. H. *et al.* Nucleic acid aptamers: An emerging tool for biotechnology and biomedical sensing. *Sensors* **15**, 16281–16313 (2015).
16. Tuerk, C. & Gold, L. Systematic evolution of ligands by exponential enrichment: RNA ligands to bacteriophage T4 DNA polymerase. *Science* **249**, 505–10 (1990).
17. Robertson, D. L. & Joyce, G. F. Selection in vitro of an RNA enzyme that specifically cleaves single-stranded DNA. *Nature* **344**, 467–468 (1990).
18. Ellington, A. D. & Szostak, J. W. In vitro selection of RNA molecules that bind specific ligands. *Nature* **346**, 818–822 (1990).
19. McKeague, M. *et al.* Analysis of In Vitro Aptamer Selection Parameters. *J. Mol. Evol.* **81**, 150–161 (2015).
20. Fu, Z., Lu, Y.-C. & Lai, J. J. Recent Advances in Biosensors for Nucleic Acid and Exosome Detection. *Chonnam Med. J.* **55**, 86 (2019).
21. Song, S., Wang, L., Li, J., Fan, C. & Zhao, J. Aptamer-based biosensors. *TrAC - Trends Anal. Chem.* **27**, 108–117 (2008).
22. Lafontaine, D. *et al.* Selection and Biosensor Application of Aptamers for Small Molecules. *Front. Chem.* **1**, 25 (2016).
23. Hanif, A. *et al.* Aptamer based nanobiosensors: Promising healthcare devices. *Saudi Pharmaceutical Journal* **27**, 312–319 (2019).
24. Taylor, A. I., Arangundy-Franklin, S. & Holliger, P. Towards applications of synthetic genetic polymers in diagnosis and therapy. *Current Opinion in Chemical Biology* **22**, 79–

84 (2014).

25. Zhang, Y., Lai, B. S. & Juhas, M. Recent advances in aptamer discovery and applications. *Molecules* (2019).
26. Keefe, A. D., Pai, S. & Ellington, A. Aptamers as therapeutics. *Nat. Publ. Gr.* (2010).
27. Herdewijn, P. & Marlière, P. Toward safe genetically modified organisms through the chemical diversification of nucleic acids. *Chem. Biodivers.* **6**, 791–808 (2009).
28. Steele, F. R. & Gold, L. The sweet allure of XNA. *Nature Biotechnology* **30**, 624–625 (2012).
29. Rose, K. M. *et al.* Selection of 2′-Deoxy-2′-Fluoroarabino Nucleic Acid (FANA) Aptamers That Bind HIV-1 Integrase with Picomolar Affinity. (2019).
30. Burmeister, P. E. *et al.* Direct in vitro selection of a 2′-O-methyl aptamer to VEGF. *Chem. Biol.* **12**, 25–33 (2005).
31. Rangel, A. E., Chen, Z., Ayele, T. M. & Heemstra, J. M. In vitro selection of an XNA aptamer capable of small-molecule recognition. *Nucleic Acids Res.* **46**, 8057–8068 (2018).
32. Anosova, I. *et al.* Structural Insights into Conformation Differences between DNA/TNA and RNA/TNA Chimeric Duplexes. *ChemBioChem* **17**, 1705–1708 (2016).
33. Mei, H. *et al.* Synthesis and Evolution of a Threose Nucleic Acid Aptamer Bearing 7-Deaza-7-Substituted Guanosine Residues. (2018).
34. Yu, H., Zhang, S., Dunn, M. R. & Chaput, J. C. An efficient and faithful in vitro replication system for threose nucleic acid. *J. Am. Chem. Soc.* **135**, 3583–3591 (2013).
35. Ichida, J. K. *et al.* An in vitro selection system for TNA. *J. Am. Chem. Soc.* **127**, 2802–2803 (2005).
36. Fiedler, J. D., Brown, S. D., Lau, J. L. & Finn, M. G. RNA-directed packaging of enzymes within virus-like particles. *Angew. Chemie - Int. Ed.* **49**, 9648–9651 (2010).
37. Yenkoidiok-Douti, L., Williams, A. E., Canepa, G. E., Molina-Cruz, A. & Barillas-Mury, C.

Engineering a Virus-Like Particle as an Antigenic Platform for a Pfs47-Targeted Malaria Transmission-Blocking Vaccine. *Sci. Rep.* **9**, 1–9 (2019).

38. Cadena-Nava, R. D. *et al.* Self-Assembly of Viral Capsid Protein and RNA Molecules of Different Sizes: Requirement for a Specific High Protein/RNA Mass Ratio. (2012).
39. Hassani-Mehraban, A., Creutzburg, S., Heereveld, L. & Kormelink, R. Feasibility of Cowpea chlorotic mottle virus-like particles as scaffold for epitope presentations. *BMC Biotechnol.* **15**, 1–17 (2015).
40. Steinmetz, N. F. Viral nanoparticles as platforms for next-generation therapeutics and imaging devices. *Nanomedicine: Nanotechnology, Biology, and Medicine* **6**, 634–641 (2010).
41. Singh, P. *et al.* Bio-distribution, toxicity and pathology of cowpea mosaic virus nanoparticles in vivo. *J. Control. Release* **120**, 41–50 (2007).
42. Assaf, H., Azouri, H. & Pallardy, M. Ochratoxin A Induces Apoptosis in Human Lymphocytes through Down Regulation of Bcl-xL. *Toxicol. Sci.* **79**, 335–344 (2004).
43. Petzinger, E. & Ziegler, K. Ochratoxin A from a toxicological perspective. *J. Vet. Pharmacol. Ther.* **23**, 91–98 (2000).
44. Pfohl-Leszkowicz, A. & Manderville, R. A. Ochratoxin A: An overview on toxicity and carcinogenicity in animals and humans. *Mol. Nutr. Food Res.* **51**, 61–99 (2007).
45. O'Brien, E. & Dietrich, D. R. Ochratoxin A: the continuing enigma. *Crit. Rev. Toxicol.* **35**, 33–60 (2005).
46. McKeague, M. *et al.* Selection and Characterization of a Novel DNA Aptamer for Label-Free Fluorescence Biosensing of Ochratoxin A. *Toxins (Basel).* **6**, 2435–2452 (2014).
47. Han, K., Liang, Z. & Zhou, N. Design strategies for aptamer-based biosensors. *Sensors* **10**, 4541–4557 (2010).
48. Feagin, T. A., Maganzini, N. & Soh, H. T. Strategies for Creating Structure-Switching Aptamers. *ACS Sensors* **3**, 1611–1615 (2018).

49. Tan, Z., Feagin, T. A. & Heemstra, J. M. Temporal Control of Aptamer Biosensors Using Covalent Self-Caging to Shift Equilibrium. *J. Am. Chem. Soc.* **138**, 6328–6331 (2016).

50. Liljeström, V., Mikkilä, J. & Kostiainen, M. A. Self-assembly and modular functionalization of three-dimensional crystals from oppositely charged proteins. *Nat. Commun.* **5**, (2014).

51. Comellas-Aragonès, M. *et al.* A virus-based single-enzyme nanoreactor. *Nat. Nanotechnol.* **2**, 635–639 (2007).

52. Ravasco, J. M. J. M., Faustino, H., Trindade, A. & Gois, P. M. P. Bioconjugation with Maleimides: A Useful Tool for Chemical Biology. *Chem. – A Eur. J.* **25**, 43–59 (2019).

53. Speir, J. A. *et al.* Enhanced local symmetry interactions globally stabilize a mutant virus capsid that maintains infectivity and capsid dynamics. *J.Virol.* **80**, 3582–3591 (2006).

54. Lavelle, L., Michel, J. P. & Gingery, M. The disassembly, reassembly and stability of CCMV protein capsids. *J. Virol. Methods* **146**, 311–316 (2007).

55. Gillitzer, E., Willits, D., Young, M. & Douglas, T. Chemical modification of a viral cage for multivalent presentation. *Chem. Commun.* **2**, 2390–2391 (2002).